Supplementary material

Beta oscillations precede joint attention and correlate with mentalization in typical development and autism

Patricia Soto-Icaza*[1], Lorena Vargas[3], Francisco Aboitiz[1], Pablo Billeke*[2]

[1] Laboratorio de Neurociencias Cognitivas, Departamento de Psiquiatría, Centro Interdisciplinario de Neurociencias, Facultad de Medicina, Pontificia Universidad Católica de Chile.

[2] División de Neurociencias, Centro de Investigación en Complejidad Social (neuroCICS), Facultad de Gobierno, Universidad del Desarrollo, Santiago, Chile.

[3] Hospital Luis Calvo Mackenna, Santiago, Chile.

*Address correspondence to Patricia Soto-Icaza, PhD., Laboratorio de Neurociencias Cognitivas, Departamento de Psiquiatría, Facultad de Medicina, Pontificia Universidad Católica de Chile, Marcoleta 391, Santiago 8330024, Chile, pasoto@uc.cl and Pablo Billeke, PhD., División de Neurociencias, Centro de Investigación en Complejidad Social (neuroCICS), Facultad de Gobierno, Universidad del Desarrollo, Av. Las Condes 12461, Las Condes, Santiago 7590943, Chile, pbilleke@udd.cl

EEG Analysis and Modeling

Time frequency (TF) distributions were obtained by means of the wavelet transform during a time-windows placed between -0.5 s and 1 s about the stimuli. Thus, the signal (the time series) x(t) was convolved with a complex Morlet's wavelet function defined by:

$$w(t, f_0) = Ae^{-t^2/2\sigma_t^2} e^{i2\pi f_0 t} . \quad (1)$$

The normalization factor A was set to $A = (\sigma_t \sqrt{\pi})^{-1/2}$. The width $m = f_o / \sigma_f$ of each wavelet function was chosen as 5, where $\sigma_f = \frac{1}{2}\pi\sigma_t$.

TF contents were represented as the energy of the convolved signal:

$$E(t, f_0) = \left| w(t, f_0) \otimes x(t) \right|^2 . \quad (2)$$

Thus, we obtained the phase and amplitude per each temporal (in steps of 5 ms) frequency (from 1 to 30 Hz in step of 1 Hz) bin. We used all of the artifact-free single trials for the modeling. For all of the TF analyses, we used the dB of power related to a baseline.

We computed the models for each subject based on the single trial wavelet transform (first-level analysis). Thus, we computed one model for the TD study and another one for TD and ASD study.

The following is the model for TD study:

$$Power\ (f,t)\ = b_1\ + b_2\ JA + b_3\ pJA + b_4\ JA * pJA \quad (3)$$

where *Power (f,t)* represents the spectral power for the frequency *f* (ranging from 5 to 45 Hz) and time *t* (ranging from -0.3 to 1 s), *JA* is a Boolean regressor that takes the value 1 if a JA occurred in the trial, *pJA* is a Boolean regressor that takes the value 1 if a JA occurred in the preceding trial, and b_x is the corresponding estimated slope. This model separates a cluster of behaviors in the first JA from behaviors in a JA preceded by another JA.

Another model was used to specifically isolate the activity of the first JA trials. This model has only two regressor, as follows:

$$Power\ (f,t) = b_1 + b_2\ First\_JA + b_3\ JA \qquad (4)$$

where *Power (f,t)* represents the spectral power for the frequency *f* (ranging from 5 to 45 Hz) and time *t* (ranging from -0.3 to 1 s), *First JA* is a Boolean regressor that takes the value 1 if the first JA of a sequence of JA behavior occurred in the trial, *JA* is a Boolean regressor that takes the value 1 if a JA occurred in the current trial, and b_x is the corresponding estimated slope.

Thus, per each regressor and subject, we obtained a three-dimensional matrix (time, frequency, electrode) which we used in the second-level analysis. In this analysis, we compared each bin of the preceding matrices across subjects. We carried out the following three types of comparisons:

1) We explored for consistent modulations within the same condition and group. For this, we used the Wilcoxon signed sum test, evaluating whether the means were other than zero.
2) We explored for modulations between the conditions within the same group. For this, we used the Wilcoxon signed sum test, evaluating whether the differences of the mean were other than zero.
3) We explored for modulations between the groups. For this, we used the Wilcoxon sum rank test, evaluating whether the differences of the means were other than zero for non–paired samples.

Using the cluster based permutation test [1], all of the results were corrected for multiple comparisons.

The modeling employed offers a number of advantages over classical categorical analysis. We used the T-value, which represents the mean (slope) normalized by the standard error, and included inter-individual variation in the analysis, thus improving the statistical inference. Classical categorical analysis uses only the mean per condition, which is more sensitive to outliers and noise (for an example, see the results in the Supplementary Material in Billeke et al., 2015 [2]).

Permutation Test

In order to correct for multiple comparison in the time-frequency analysis, we carried out the cluster based permutation test [1]. In this test, clusters of significant areas were defined by pooling neighboring sites (bins of time-frequency-electrode matrices or sources) that showed the same effect ($p < 0.05$ in the statistical test carried out in the sites of either the time-frequency chart or the sources, e.g., the Wilcoxon test). The cluster-level statistics was computed as the sum of the statistics of all sites within the corresponding cluster. We evaluated the cluster-level significance under the permutation distribution of the cluster that had the largest cluster-level statistics. The permutation distribution was obtained by randomly permuting the original data. After each permutation, the original statistical test was computed (e.g., the Wilcoxon test). For the permutation distribution, we used the cluster-level statistics of the largest cluster which resulted after each permutation. After 1,000 permutations, the cluster-level significance of each observed cluster was estimated as the proportion of elements of the permutation distribution greater than the cluster-level statistics of the corresponding observed cluster.

Source Estimations

We estimated the neural current density time series at each elementary brain location applying a weighted minimum norm estimate inverse solution with unconstrained dipole orientations in single trials per condition per subject. We used q tessellated cortical mesh template surface derived from a template for 3-year-old children (Neurodevelopmental MRI Database of the University of South Carolina [3]). The location of the electrodes (HGCSN 64) was the average location of the children from whom the MRI Database was made. We defined 3 x 4000 sources constrained to the segmented cortical surface (3 orthogonal sources at each spatial location), and we computed both a three-layer (scalp, inner skull, outer skull) boundary element conductivity model and the physical forward model. The measured electrode level data $X(t) = \left[x_1(t), \cdots, x_{n\_electrode}(t) \right]$ is assumed to be linearly related to a set of cortical sources $Y(t) = \left[y_1(t), \cdots, y_{m\_source}(t) \right]$ (3 x 5005 sources, see above) and to an additive noise $N(t) : X(t) = LY(t) + N(t)$, where L is the physical forward model. The inverse solution was then derived as $Y(t) = WX(t) = RL^T (LRL^T + \lambda^2 C)^{-1} X(t)$, where W is the inverse operator, R and C are the source and noise covariance, respectively, and λ is the regularization parameter. R is the identity matrix that was modified to implement depth-weighing (weighing exponent 0.8). The regularization parameter λ was set to 1/3. The noise covariance matrix among the electrodes (C) was independently calculated for the ERP signal (using the average signal) and for TF analysis (using single-trial signal). To estimate cortical activity at the cortical sources, the recorded raw EEG time series at the sensors x(t) were multiplied by the inverse operator W to yield the estimated source current as a function of

time at the cortical surface $Y(t) = WX(t)$. Since this is a linear transformation, it does not modify the frequencies of the underlying sources. It is, therefore, possible to undertake time–frequency analysis on the source space directly. In this source space, we computed frequency decomposition using the Wavelets transform as in the scalp levels (see above). Since we used a small number of electrodes and no individual anatomy for head model calculation, the spatial precision of the source estimations was limited. In order to provide more information about the localization procedure, for all source estimations, we show the scalp distribution of activity computed separately from the electrode space. Finally, in order to minimize the possibility of erroneous results, we present only source estimations in the case where there are both statistically significant differences at the electrode level and the differences at the source levels survive a multiple comparison correction.

References

1. Maris, E. & Oostenveld, R. Nonparametric statistical testing of EEG- and MEG-data. *J Neurosci Methods* **164,** 177–190 (2007).
2. Billeke, P. *et al*. Paradoxical Expectation: Oscillatory Brain Activity Reveals Social Interaction Impairment in Schizophrenia. *Biol. Psychiatry* **78,** 421–31 (2015).
3. Sanchez, C. E., Richards, J. E. & Almli, C. R. Neurodevelopmental MRI brain templates for children from 2 weeks to 4 years of age. *Dev. Psychobiol.* **54,** 77–91 (2012).

Supplementary Figures

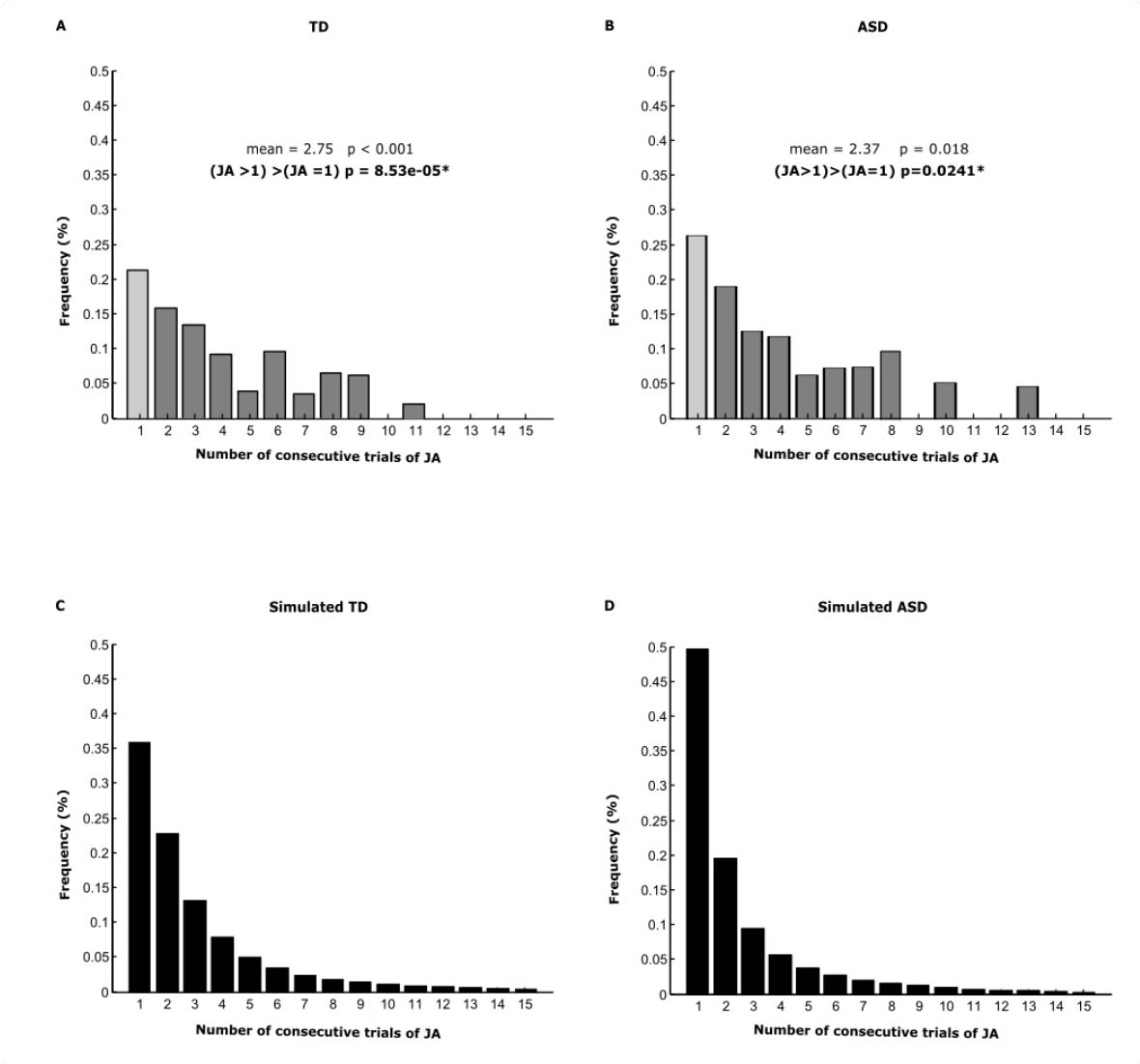

Supplementary Figure 1: Percentage of frequency of JA behaviors that occur in isolation (light grey) **and consecutively** (dark grey) in the **(A)** TD group of children, **(B)**

ASD group of children, **(C)** Simulated TD children and **(D)** simulated ASD children. The asterisk (*) indicates a statistically significant difference.

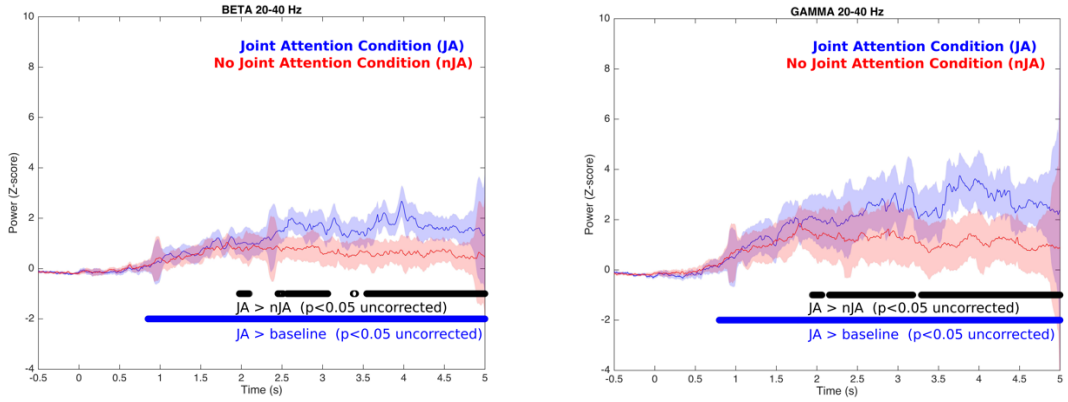

<u>Supplementary Figure 2</u>: Time course of the amplitudes of broadband beta and gamma ranges as a proxy of EMG activity (occipital and temporal electrodes). Blue lines represent Joint attention (JA) condition and red lines no joint attention (nJA) condition. Blue rectangles represent significant differences between JA and baseline (Wilcoxon test, one-tail, $p < 0.05$ uncorrected). Black rectangles represent significant differences between JA and nJA conditions (Wilcoxon test, one-tail, $p < 0.05$ uncorrected). Error areas represent 95% confidence intervals.

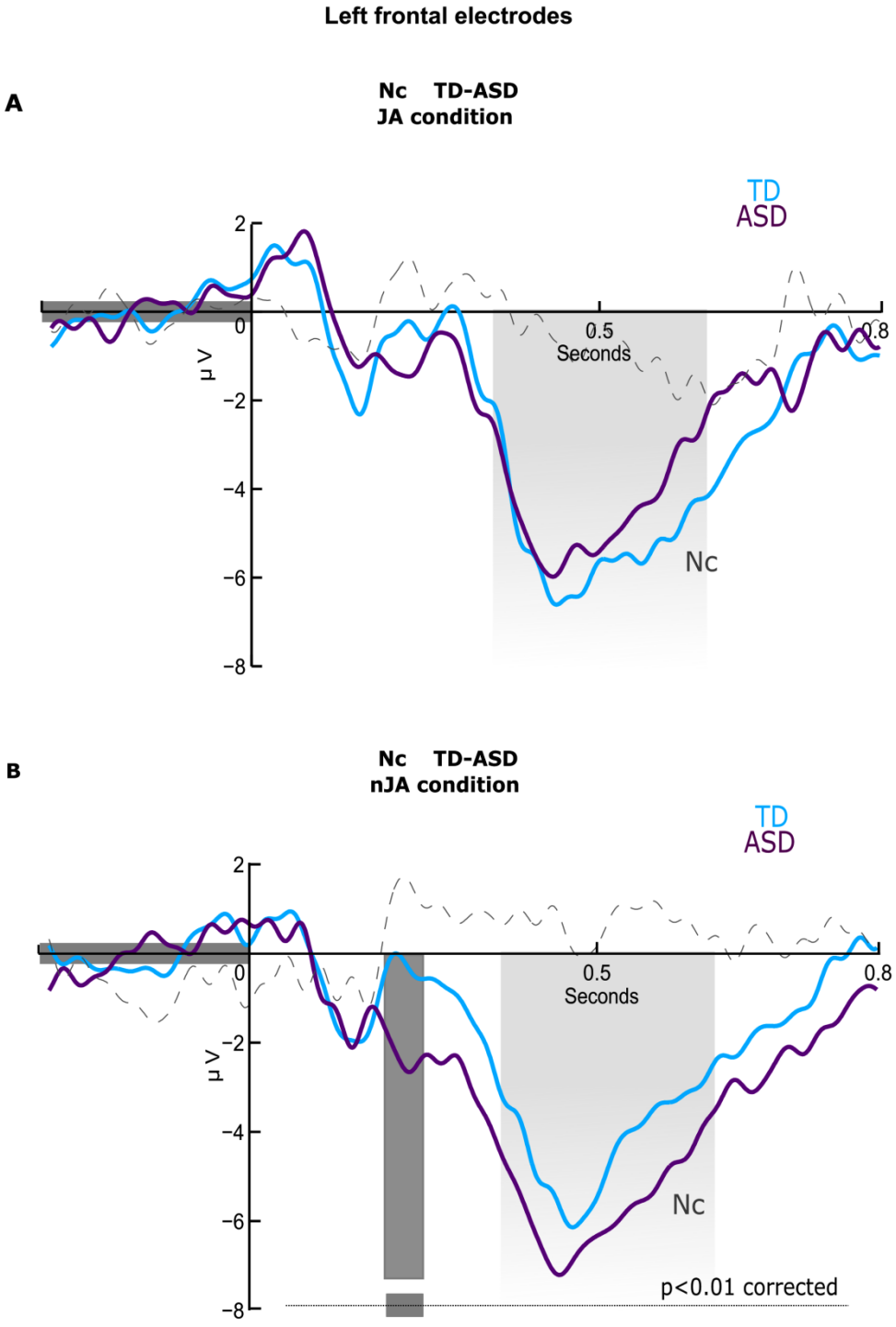

<u>Supplementary Figure 3</u>: Electrical brain activity of the difference in left central electrodes in TD and ASD groups of children in (A) JA condition and in **(B)** nJA condition.

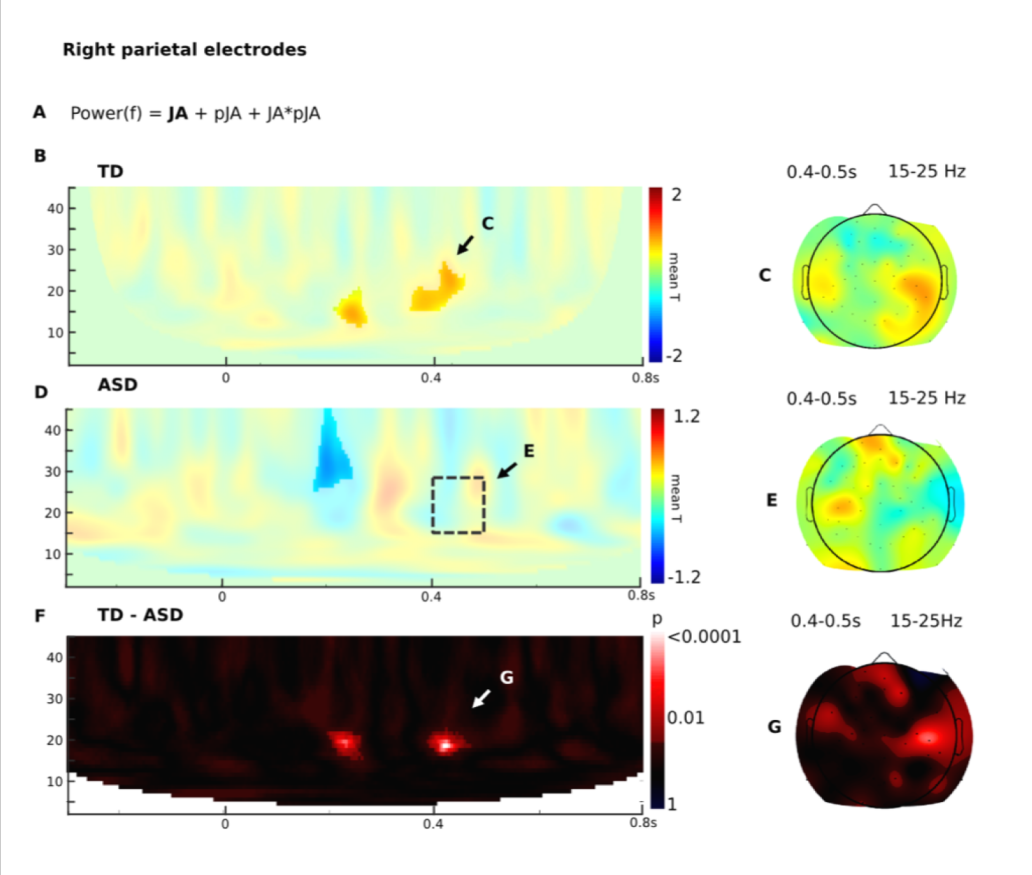

<u>Supplementary Figure 4</u>: Oscillatory brain activity in the TD and the ASD groups during the JA trial. **(A)** Model used to estimate the modulation of the JA. **(B)** Time–frequency chart of the JA regressor in TD children in right parietal electrodes. **(C)** Topographic distribution of the significant cluster of beta activity (15 Hz – 25 Hz, 0.4 s – 0.55 s) as shown in (B)**. (D)** Time–frequency chart of the JA regressor in the ASD group in right parietal electrodes. The dotted line rectangle indicates the region of the significant cluster found in TD children. **(E)** Topographic distribution of the significant cluster of beta activity (15 Hz – 25 Hz, 0.4 s – 0.55 s) as shown in (D) using the same cluster found in TD children shown in (B). **(F)** Time–frequency chart of the p-values of the difference between the TD group and the ASD group in the oscillatory activity of the JA regressor. **(G)** Scalp distribution of p-values of the difference between groups as shown in (E).

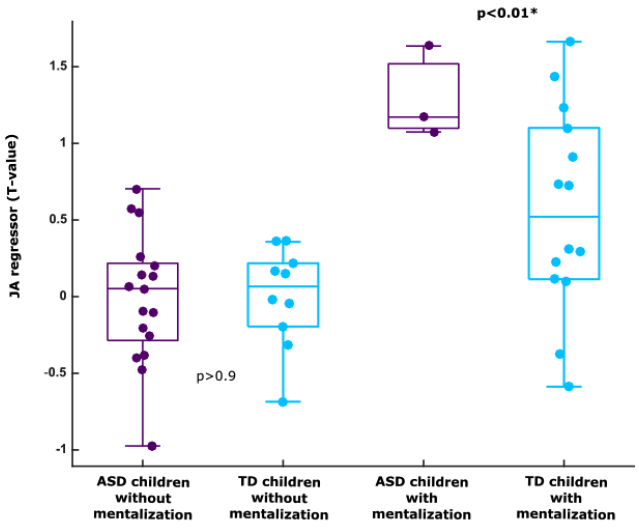

<u>Supplementary Figure 5</u>: Comparison of the cerebral activity in the temporo-parietal region of JA condition in both group of children who evidenced explicit mentalization and children who do not evidence it. Light blue circles are TD participants and purple circles are ASD participants. *Asterisk (*) indicates statistically significant difference ($p < 0.05$ Wilcoxon test).*

<u>Supplementary Table 1</u>: Spearman Partial Correlation among TJP beta activity, mentalization and frequency of isolate JA in TD children (n=24).

Rho(p-value)	Beta TPJ	Freq. of isolate JA
Pass SA task	**0.44 (0.03)**	0.08 (0.69)
Beta TPJ		0.43 (0.04)

<u>Supplementary Table 2</u>: Spearman Partial Correlation among TJP beta activity, IPS beta activity, age, mentalization and frequency of isolate JA in TD children (n=24).

Rho(p-value)	Beta TPJ	Beta IPS	Age	Freq. of isolate JA
Pass SA task	**0.58 (0.005)**	-0.5 (0.019)	0.51 (0.016)	-0.06 (0.7)
Beta TPJ		0.89 (<0.001)	-0.044 (0.04)	0.49 (0.02)
Beta IPS			0.5 (0.18)	-0.34 (0.1)
Age				0.1 (0.6)

Supplementary Table 3: Spearman Partial Correlation among EEG marker and behavioral variables in ASD children (n=20).

Rho(p-value)	ADOS-score	Beta TPJ	Mentalization
Nc (left frontal)	-.48 (0.043)	-0.3 (0.2)	0.47 (0.46)
ADOS-score		-.15(0.5)	0.18 (0.4)
Beta TPJ			0.66 (0.002)